

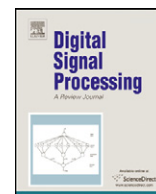


ELSEVIER

Contents lists available at ScienceDirect

## Digital Signal Processing

www.elsevier.com/locate/dsp



## Unitary design of radar waveform diversity sets

Tariq R. Qureshi<sup>a</sup>, Michael D. Zoltowski<sup>a,\*</sup>, Robert Calderbank<sup>b</sup>, Ali Pezeshki<sup>c</sup><sup>a</sup> School of Electrical Engineering, Purdue University, West Lafayette, IN 47907, United States<sup>b</sup> Department of Electrical Engineering, Princeton University, Princeton, NJ 08544, United States<sup>c</sup> Department of Electrical Engineering, Colorado State University, CO 80523, United States

## ARTICLE INFO

## Article history:

Available online xxxx

## Keywords:

Ambiguity function

Unitary waveform design

Multiple antennas

Doppler compensation

## ABSTRACT

In this work, multiple radar waveforms are simultaneously transmitted, emitted from different antennas. The goal is to process the returns in such a way that the overall ambiguity function is a sum of individual ambiguity functions, such that the sum better approximates the ideal thumbtack shape. A unitary design for the illustrative  $4 \times 4$  example prescribes the scheduling of the waveforms over four transmit antennas over four PRIs. Further, it dictates how the matched filtering of the returns over four PRIs is combined in such a way so as to achieve both perfect separation (of the superimposed returns) AND perfect reconstruction. Perfect reconstruction implies that the sum of the time-autocorrelations associated with each of the four waveforms is a delta function. The net result of the processing of four PRIs over four virtual antennas yields 16 cross-correlations all of which ideally exhibit a sharp peak at the target delay. Conditions for both perfect separation and perfect reconstruction are developed, and a variety of waveform sets satisfying both are presented. Doppler compensation is achieved by a data-dependent weighting of the different PRI matched-filtered outputs prior to summing. Simulations are presented verifying the efficacy of the proposed unitary waveform matrix designs in conjunction with the proposed Doppler compensation technique.

© 2010 Published by Elsevier Inc.

## 1. Introduction

In active sensing systems, the objective is to design a communication system that allows one to learn the environment, which could be one or more moving targets in the case of a radar. In a radar system, the transmitted waveforms are reflected by the target and the reflected returns are then processed at the receiving end to determine the location and speed of the target. The delay in the received waveforms corresponds to the distance of the target from the radar, and the Doppler shift determines the speed at which the target is moving [1]. Therefore, it is desired to transmit a waveform that provides good resolution in terms of the delay–Doppler properties of the radar returns. This is characterized by the use of ambiguity functions, which measure the delay–Doppler correlation of the received waveforms with the actual transmitted waveform. The ambiguity function [1] of a waveform  $s(t)$  is given by

$$\chi(\tau, \nu) = \int_{-\infty}^{\infty} s(t)s^*(t - \tau)e^{-j2\pi\nu t} dt \quad (1)$$

\* Corresponding author.

E-mail addresses: tqureshi@ecn.purdue.edu (T.R. Qureshi), mikedz@ecn.purdue.edu (M.D. Zoltowski), calderbk@princeton.edu (R. Calderbank), pezeszki@engr.colostate.edu (A. Pezeshki).

where  $\tau$  and  $\nu$  are the delay and the Doppler shift respectively. A perfect radar waveform would have the ambiguity function that satisfies

$$\chi(\tau, \nu) \propto \delta(\tau)\delta(\nu) \quad (2)$$

which means that the spike in the ambiguity function would correspond to the correct delay and Doppler properties of the target. However, waveforms with this kind of ambiguity function do not exist [1]. However, it should be noted that for correct target detection, waveforms with a thumbtack shaped ambiguity function are not always necessary. In particular, if there is only one target or if there are multiple targets that are reasonably well separated in the delay–Doppler domain, a waveform with ambiguity function that decays sufficiently fast in delay–Doppler so as to not confuse the nearby targets is sufficient.

In radar systems, the advantages of using closely-spaced antennas at the receivers are well known [2–4], some of which are electronic steerability of the antenna array and the ability to use array processing techniques for improved detection. Recently, there has been a lot of interest in radars employing multiple antennas at both the transmitter and the receiver. These radars are commonly known as MIMO (Multiple Input Multiple Output) radars. MIMO radar [5] offers superior performance over the conventional radar systems in that it provides multiple independent views of the target if the antennas are placed sufficiently far apart. In an MIMO radar, different waveforms are transmitted from the transmitting antennas and the returns are then processed to determine the target presence, location and speed. The challenge in MIMO radar, among other things, is waveform separation at the receiver. To this end, a widely studied approach has been to transmit orthogonal waveforms that can be separated at the receiver. However, the relative delay and Doppler shift of the transmitted waveforms might destroy their orthogonality, and therefore, we need waveforms that remain orthogonal through a certain range of delay and Doppler shifts. The design of such waveforms has been studied extensively in the context of CDMA (Code Division Multiple Access) systems [6].

In [7], Howard et al. proposed a new multi-channel radar scheme employing polarization diversity for getting multiple independent views of the target. In this scheme, Golay pairs [8] of phase coded waveforms are used to provide synchronization and Alamouti [9] coding is used to co-ordinate transmission of these waveforms on the horizontal and vertical polarizations. The combination of Golay complementary sequences and Alamouti coding makes it possible to do radar ambiguity polarimetry on a pulse-by-pulse basis, which reduces the signal processing complexity as compared to distributed aperture radar. This scheme [7] has been shown to provide the same detection performance as the single channel radar with significantly smaller transmit energy, or provide detection over greater ranges with the same transmit energy as the single channel radar.

The work done by Howard et al. [7] is based on processing the transmitted waveform matrix – which represents the scheduling of individual waveforms over space and time – at the receiver in a manner that allows us to separate the transmitted waveforms at the receiver and exploit the diversity inherent in an active sensing environment due to its multipath nature. In [7], the waveform separation was achieved through the use of Golay complementary sequences. In this paper, multiple radar waveforms are simultaneously transmitted from different “virtual antenna” elements over multiple PRIs (Pulse Repetition Intervals) where each antenna element is a transceiver. The goal is to process the returns in such a way that the overall ambiguity function is a sum of individual ambiguity functions, such that the sum better approximates the desired thumbtack shape. The use of the term “virtual antenna” here can also include simultaneous beams formed from the same aperture but pointed to different angles, or beams pointed to the same angle but formed from different sub-apertures. We present an example of a  $4 \times 4$  system with two dually polarized transceivers. A  $4 \times 4$  unitary design implies the following features. First, it dictates the scheduling of the waveforms over the four virtual antennas over four PRIs. Secondly, it tells us how the matched filtering of the returns over four PRIs are combined in such a way so as to achieve both perfect separation (of the superimposed returns) and perfect reconstruction. Perfect reconstruction implies that the sum of the time-autocorrelations associated with each of the four waveforms is a delta function. Perfect separation is needed because waveforms from different antennas interfere, and we want to design waveform matrices that achieve perfect separation so that there is no inter-waveform interference. The net result of the processing of four PRIs over four virtual antennas yields sixteen cross-correlations all of which ideally exhibit a sharp peak at the target delay.

In the case of a moving target, however, delay resolution of a waveform is not enough for accurate target ranging, because the autocorrelation may have significant sidelobes along the non-zero Doppler axis. Therefore, any waveform design scheme needs to ensure that it performs well in the presence of Doppler. This is one of the main reasons that complementary sequences haven't found a widespread use in the radar literature in the past; they don't perform well in the presence of Doppler. In [10], PTM [11–15] sequences were used to make the Golay sequence transmissions resilient against Doppler shifts. The method achieves good results for small Doppler shifts, but the number of PRIs needed per transmission of the coded Golay sequence matrix is large, and would only work for slow moving targets. In this paper, we describe another Doppler compensation method that exploits the subspace structure of the transmitted waveform matrix. We show that the received waveform matrix can be processed in a way that imparts a specific structure on the subspace that it occupies, and the null-space of this matrix can be used to minimize the effects of Doppler. We develop a processing filter using the null-space of this matrix to alleviate the effects of Doppler in target ranging, and show that the method works over a wide range of target SNRs.

## 2. System model

We consider a system with  $N$  transmit and receive antennas, and we refer to it as an  $N \times N$  system from here on in. We assume that the distance between the target and the transmit/receive antennas is large enough to make the point target assumption valid. There is a loose time co-ordination between the transmitter and the receiver, in that the received waveforms differ only by a constant phase factor, i.e. if the transmitted waveform from the  $i$ th antenna is  $s(t)$ , then the received waveform at the  $k$ th antenna is given by

$$r_k(t) = h_{ik} e^{j\phi_{ik}} s(t - \tau) \quad (3)$$

where  $h_{ik}$  is the path gain and  $\phi_{ik}$  is the random phase between the  $i$ th transmit antenna and the  $j$ th receive antenna, and  $\tau$  is the delay which is assumed to be constant between all transmit and receive antenna pairs. Since  $\phi_{ik}$  is only a phase factor, we can absorb it in the path gain. The delay is given by  $\tau = \frac{d_T + d_R}{c}$  where  $d_T$  is the distance from the transmitter(s) to the target, and  $d_R$  from the target to the receiver(s). The relative motion between the target and the transmitter/receiver introduces a Doppler shift, which under certain conditions can be modeled as a phase shift between successive PRIs, i.e., if we transmit the same waveform in adjacent PRIs, the received waveforms in the second PRI is just a phase shifted version of the waveform in the first PRI. Notice that we have implicitly assumed that the path gain  $h_{ik}$  stays constant for adjacent PRIs. This assumption is valid if the system is designed such that the target range and velocity does not change appreciably over the transmission of  $N$  pulses.

We are now ready to develop the system equation for our  $N \times N$  MIMO radar. The  $N \times N$  waveform matrix  $\mathbf{S}(n)$  is transmitted from the  $N$  transmit antennas over  $N$  PRIs, giving the system equation

$$\mathbf{R}(n) = \sum_{k=1}^M \mathbf{H}_k \mathbf{S}(n - d_k) \mathbf{D}_k + \mathbf{N}(n) \quad (4)$$

where  $k$  is the target index,  $n$  is the chip index within a pulse,  $\mathbf{R}(n)$  is the  $N \times N$  receive waveform matrix, where the rows represent antennas and columns represent PRIs.  $\mathbf{H}_k$  is the channel matrix for the  $k$ th target with individual entries of the form

$$[\mathbf{H}_k]_{ij} = h_{ij}^{(k)} \quad (5)$$

and  $\mathbf{D}_k$  is the matrix that represent the phase shifts due to Doppler between PRIs, and is given by

$$\mathbf{D}_k = \text{diag}(1, e^{j\nu_k}, \dots, e^{j(N-1)\nu_k}) \quad (6)$$

and  $\mathbf{N}(n)$  is the noise matrix with i.i.d. zero mean Gaussian entries with variance  $\sigma_n^2$ . The problem is to design the matrix  $\mathbf{S}(n)$  that would allow us to extract the maximum information about the target scene. To this end, we'll assume for now that we are dealing with a single target and that the Doppler shift is negligible, resulting in  $\mathbf{D} = \mathbf{I}$ , and present some waveform designs for the special cases of  $2 \times 2$  and  $4 \times 4$  systems. We'll later show how these designs can be generalized to multiple targets with different Doppler shifts and systems with arbitrary antenna dimensions.

## 3. Unitary waveform matrices

As stated in the previous section, we are interested in designing the matrix  $\mathbf{S}(n)$  to extract maximum information about the target scene. To do this, one choice would be orthogonal sequences, however, it is difficult to design sequences that are orthogonal over a range of delays. As opposed to the orthogonal sequences, we can consider sequences where the sum of two or more sequences goes to zero. Specifically, consider a set of  $N$  sequences satisfying

$$\sum_{i=1}^N s_i(n) * s_i^*(-n) = N\delta(n) \quad (7)$$

We will use these waveforms to construct unitary waveform matrices. For now, we consider  $N$  such that  $N = 2^m$  where  $m \in \mathbb{N}$ . Let us first consider the case  $m = 1$  and look at the waveform matrix  $\mathbf{S}(n)$ , which was developed in [7], and is given by

$$\mathbf{S}_2(n) = \begin{bmatrix} s_1(n) & s_2^*(-n) \\ s_2(n) & -s_1^*(-n) \end{bmatrix} \quad (8)$$

Now, if we define

$$\mathbf{S}_2^H(-n) = \begin{bmatrix} s_1^*(n) & s_2^*(-n) \\ s_2(n) & -s_1(n) \end{bmatrix} \quad (9)$$

we immediately see that

$$\mathbf{S}_2(n) * \mathbf{S}_2^H(-n) = 2\mathbf{I}_2\delta(n) \quad (10)$$

It is interesting to look at the structure of these matrices in the frequency domain. In particular, the above convolution operation would be transformed in the frequency domain as

$$\mathbf{S}_2(\omega)\mathbf{S}_2^H(\omega) = \begin{bmatrix} S_1(\omega) & S_2^*(\omega) \\ S_2(\omega) & -S_1^*(\omega) \end{bmatrix} \begin{bmatrix} S_1^*(\omega) & S_2^*(\omega) \\ S_2(\omega) & -S_1(\omega) \end{bmatrix} \quad (11)$$

Now, taking the DFT of (7), we get

$$\sum_{i=1}^N S_i(\omega)S_i^*(\omega) = N \quad (12)$$

which gives

$$\mathbf{S}_2(\omega)\mathbf{S}_2^H(\omega) = 2\mathbf{I}_2 \quad (13)$$

As we can see from this equation, the DFT of the transmitted waveform matrix is a unitary matrix for all digital frequencies  $\omega \in [-\pi, \pi)$ . We can also observe that this frequency domain waveform matrix represents a  $2 \times 2$  design. Now, consider waveform matrix design for  $N \times N$  systems such that  $N$  is a power of two:  $N = 2^k$ ,  $k \in \{1, 2, 3, \dots\}$ . Consider the  $2 \times 2$  matrix  $\mathbf{S}_2(\omega)$ . The  $4 \times 4$  and  $8 \times 8$  systems can be obtained from the  $2 \times 2$  design as follows

$$\mathbf{S}_4(\omega) = \begin{bmatrix} \mathbf{S}_2(\omega) & \mathbf{S}_2^H(\omega) \\ \mathbf{S}_2(\omega) & -\mathbf{S}_2^H(\omega) \end{bmatrix} \quad (14)$$

and

$$\mathbf{S}_8(\omega) = \begin{bmatrix} \mathbf{S}_4(\omega) & \mathbf{S}_4^H(\omega) \\ \mathbf{S}_4(\omega) & -\mathbf{S}_4^H(\omega) \end{bmatrix} \quad (15)$$

It can be easily verified that

$$\mathbf{S}_4(\omega)\mathbf{S}_4^H(\omega) = \mathbf{S}_4^H(\omega)\mathbf{S}_4(\omega) = 4\mathbf{I}_4 \quad (16)$$

and

$$\mathbf{S}_8(\omega)\mathbf{S}_8^H(\omega) = \mathbf{S}_8^H(\omega)\mathbf{S}_8(\omega) = 8\mathbf{I}_8 \quad (17)$$

Using the induction hypothesis, it can be shown that

$$\mathbf{S}_N(\omega) = \begin{bmatrix} \mathbf{S}_{N/2}(\omega) & \mathbf{S}_{N/2}^H(\omega) \\ \mathbf{S}_{N/2}(\omega) & -\mathbf{S}_{N/2}^H(\omega) \end{bmatrix} \quad (18)$$

Using the ideas developed in this section, we'll later design waveform matrices for systems with arbitrary dimensions.

### 3.1. Application in MIMO radar

We now use these ideas in our earlier  $N \times N$  model. For now, we assume  $N$  is a power of 2. Referring to (4), we can write the channel matrix for the  $k$ th target as

$$\mathbf{H}_k^T(n - d_k) = \mathbf{H}_k^T * \delta(n - d_k)\mathbf{I} \quad (19)$$

For the moment, we consider the system without Doppler, which gives the received waveform matrix as

$$\mathbf{R}(n) = \sum_{k=1}^M \mathbf{H}^T(n - d_k) * \mathbf{S}(n) \quad (20)$$

which is matched filtered at the receiver and the outputs are given by

$$\mathbf{Y}(n) = \mathbf{S}_N^*(-n) * \mathbf{R}^T(n) \quad (21)$$

This can be expanded as

$$\mathbf{Y}(n) = \{\mathbf{S}_N^*(-n) * \mathbf{S}_N^T(n)\} * \sum_{k=1}^M \mathbf{H}(n - d_k) \quad (22)$$

We know from our earlier discussion that

$$\mathbf{S}_N(n) * \mathbf{S}_N^H(-n) = N\mathbf{I}\delta(n) \quad (23)$$

Taking the transpose of this equation, we get

$$\mathbf{S}_N^*(-n) * \mathbf{S}_N^T(n) = N\mathbf{I}\delta(n) \quad (24)$$

which, when used in (22), gives

$$\mathbf{Y}(n) = \sum_{k=1}^M \mathbf{H}(n - d_k) \quad (25)$$

which shows that the use of these waveforms allows us to process them in a way where the output peaks at the correct target delays, and is zero at all other delay values if we ignore the effects of noise. In the next section, we focus on the  $4 \times 4$  system in more detail, and derive some interesting properties that would help us design waveforms that satisfy (23).

#### 4. $4 \times 4$ space–time diversity waveform design

In this section, we explore the  $4 \times 4$  design in more detail.

##### 4.1. Conditions for perfect reconstruction and separation

On possible scheduling scheme for the  $4 \times 4$  design is given by

$$\mathbf{S}(n) = \begin{bmatrix} s_1(n) & s_2^*(-n) & s_3(n) & s_4^*(-n) \\ -s_2(n) & s_1^*(-n) & -s_4(n) & s_3^*(-n) \\ -s_3(n) & s_4^*(-n) & s_1(n) & -s_2^*(-n) \\ -s_4(n) & -s_3^*(-n) & s_2(n) & s_1^*(-n) \end{bmatrix} \quad (26)$$

The received waveform matrix  $\mathbf{R}(n)$ , ignoring the noise component for now, is given by

$$\mathbf{R}(n) = \mathbf{H}^T(n) * \mathbf{S}(n) \quad (27)$$

At the receiver, the goal is to process  $\mathbf{R}(n)$  so as to achieve perfect separation of the waveforms. In the previous section, we saw how to achieve this separation, so we form

$$\Phi(n) = \mathbf{R}(n) * \mathbf{S}^H(-n) \quad (28)$$

which can be written as

$$\Phi(n) = \begin{bmatrix} \delta(n) & 0 & -\phi(n) & 0 \\ 0 & \delta(n) & 0 & \phi(n) \\ \phi(n) & 0 & \delta(n) & 0 \\ 0 & -\phi(n) & 0 & \delta(n) \end{bmatrix} \quad (29)$$

where

$$\phi(n) = -s_3(n) * s_1^*(-n) + s_4^*(-n) * s_2(n) + s_1(n) * s_3^*(-n) - s_2^*(-n) * s_4^*(-n) \quad (30)$$

We say that waveform design has *perfect reconstruction* property if

$$\theta(n) = \delta(n) \quad (31)$$

and if

$$\phi(n) = 0 \quad \forall n \quad (32)$$

we say that the waveform design has *perfect separation* property.

**Theorem 4.1.** *If the waveforms are complementary, the key matrix satisfies the perfect reconstruction property.*

**Proof.** The proof follows from (24) and the definition of  $\theta(n)$ .  $\square$

**Theorem 4.2.** *If the waveforms exhibit conjugate symmetry, or if the waveforms are time reversed versions of each other, they satisfy the perfect separation property.*

**Proof.** To prove this, we first see that  $\phi(n)$  is conjugate symmetric, i.e.,

$$\phi(-n) = -\phi^*(n) \quad (33)$$

which implies that if  $\phi(n)$  is real valued, then

$$\phi[0] = 0 \quad (34)$$

Now, we can write  $\phi(n)$  as

$$\phi(n) = (-s_3(n) * s_1^*(-n) + s_1(n) * s_3^*(-n)) + (s_4^*(-n) * s_2(n) - s_2^*(-n) * s_4^*(-n)) \quad (35)$$

From this, we can see that if all waveforms exhibit conjugate symmetry, i.e.

$$s_i(n) = s_i^*(-n) \quad (36)$$

for  $i = 1, 2, 3, 4$ , then

$$\phi(n) = 0 \quad (37)$$

and we achieve perfect separation. Also, if the waveforms are time reversed versions of each other, i.e.

$$s_1(n) = s_2^*(-n) \quad (38)$$

and

$$s_3(n) = s_4^*(-n) \quad (39)$$

then we also have

$$\phi(n) = 0 \quad (40)$$

(36) and (38) give us the conditions for perfect waveform reconstruction and separation at the receiver end. It should however, be noted that this is not an exhaustive list of conditions for perfect reconstruction and separation. Other possible conditions may still exist.  $\square$

#### 4.1.1. Working example: $4 \times 4$ radar detection

We now present an example of  $4 \times 4$  waveform design by employing a class of complementary sequences called Golay pairs. A Golay pair  $s_1(n), s_2(n)$ , is complementary for  $N = 2$ , but we can extend it to  $N = 4$  by recalling from the previous section that if the waveforms are time reversed version of each others, then they achieve perfect separation. So, we define the waveforms  $s_3(n) = s_1^*(-n)$ , and  $s_4(n) = s_2^*(-n)$ .

After receiver processing, we get the channel matrix  $\mathbf{H}$ , and we stack the entries of that matrix into a vector  $\mathbf{h} = \text{vec}(\mathbf{H})$ . The target detection problem is now transformed into a hypothesis testing problem, such that

$$T = \begin{cases} E_t \mathbf{h} + \mathbf{n}: H_1 \\ \mathbf{n}: H_0 \end{cases} \quad (41)$$

where  $\mathbf{h}$  is a  $16 \times 1$  vector of the channel coefficients that is distributed as  $CN(0, E_t \sigma^2 \mathbf{I})$  and  $\mathbf{n}$  is the noise vector with distribution  $CN(0, N_0 \mathbf{I})$ . The likelihood ratio detector is an energy detector that computes the energy in the received vector under both hypothesis and is given by

$$\|T\|^2 > \gamma \quad (42)$$

where  $\gamma$  is the detection threshold. The probability of false alarm  $P_F$  and probability of detection  $P_D$  require an investigation of the pdf of  $\|T\|^2$ , which is given by

$$f_{\|T\|^2}(t) = \begin{cases} \frac{t^{15} e^{-\frac{t}{2(E_t \sigma^2 + N_0)}}}{\{2(E_t \sigma^2 + N_0)\}^{16} (15)!}: H_1 \\ \frac{t^{15} e^{-\frac{t}{2N_0}}}{(2N_0)^{16} (15)!}: H_0 \end{cases} \quad (43)$$

and the corresponding probability of false alarm  $P_F$  and probability of detection  $P_D$  are given by

$$P_F(\gamma) = \sum_{k=0}^{15} \left( \frac{\gamma}{2N_0} \right)^k \frac{e^{-\frac{\gamma}{2N_0}}}{k!} \quad (44)$$

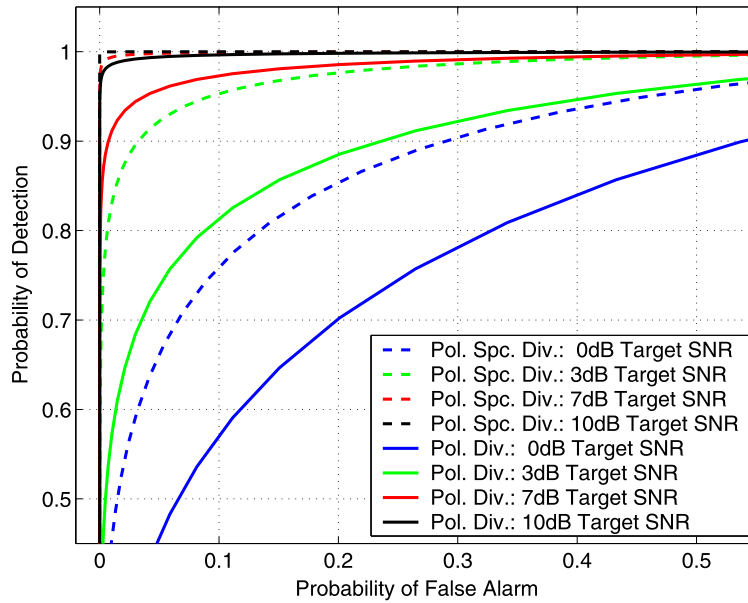


Fig. 1. Comparison of ROC curves for the  $4 \times 4$  polarization-spatial diversity and  $2 \times 2$  polarization diversity system.

and

$$P_D(\gamma) = \sum_{k=0}^{15} \left( \frac{\gamma}{2(E_t\sigma^2 + N_0)} \right)^k \frac{e^{-\frac{\gamma}{2(E_t\sigma^2 + N_0)}}}{k!} \quad (45)$$

The detection performance for the  $4 \times 4$  system is given in Fig. 1 where it is compared with the detection performance of a  $2 \times 2$  system [7]. We can see that for the same transmit energy, the performance improves with increasing the number of space-time dimensions.

### 5. Waveform families based on Kronecker products

We now develop waveform families using these Kronecker products of different sequences. Consider two pairs of complementary sequences satisfying

$$\varepsilon_1(n) * \varepsilon_1^*(-n) + \varepsilon_2(n) * \varepsilon_2^*(-n) = N_1\delta(n) \quad (46)$$

$$\varepsilon_3(n) * \varepsilon_3^*(-n) + \varepsilon_4(n) * \varepsilon_4^*(-n) = N_2\delta(n) \quad (47)$$

We form the transmitted waveforms of these sequences using the Kronecker product as

$$s_1(n) = \varepsilon_1(n) \otimes \varepsilon_3(n) \quad (48)$$

$$s_2(n) = \varepsilon_1(n) \otimes \varepsilon_4(n) \quad (49)$$

$$s_3(n) = \varepsilon_2(n) \otimes \varepsilon_3(n) \quad (50)$$

$$s_4(n) = \varepsilon_2(n) \otimes \varepsilon_4(n) \quad (51)$$

Consider forming the autocorrelation

$$r[m] = r_{s_1s_1}(m) + r_{s_2s_2}(m) + r_{s_3s_3}(m) + r_{s_4s_4}(m) \quad (52)$$

**Theorem 5.1.** *The autocorrelation  $r(m)$  possesses the complementary property of the original sequences.*

**Proof.** See Appendix A.  $\square$

We now present some waveform designs based on the results of this section.

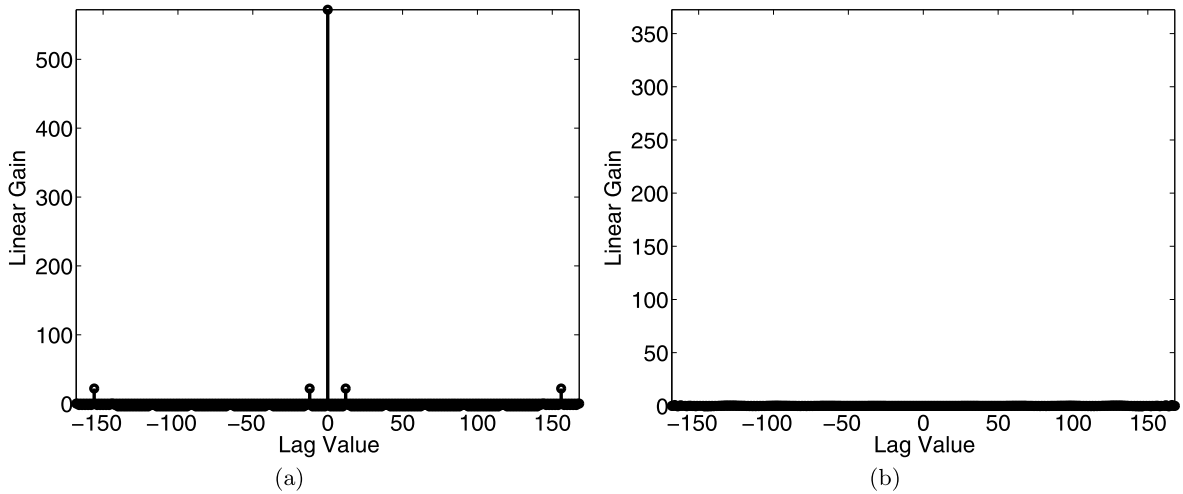


Fig. 2. (a) Main diagonal sequence: some of values around the main lobe are non-zero. (b) Off diagonal sequence is identically zero.

5.1. Kronecker products of Barker codes

Consider two Barker sequences

$$b_1(n) = \{1, 1, 1, 1, 1, -1, -1, 1, 1, -1, 1, -1, 1\}$$

$$b_2(n) = \{0, 1, 1, 1, -1, -1, -1, 1, -1, -1, 1, -1, 0\} \tag{53}$$

We form the transmitted waveforms as

$$s_1(n) = b_1(n) \otimes b_2(n)$$

$$s_2(n) = e_1^*(-n)$$

$$s_3(n) = b_2(n) \otimes b_1(n)$$

$$s_4(n) = e_3^*(-n) \tag{54}$$

These waveforms satisfy one of the conditions that leads to perfect separation given in Section 4 but their autocorrelation functions do not sum to a delta function. The diagonal and off-diagonal autocorrelation sequences are given in Figs. 2(a) and 2(b). The diagonal terms show some infrequent minor disturbances as compared to the peak, which makes these sequences an attractive choice for radar applications, even though they do not have the perfect reconstruction property in the strict sense. Because of the conjugate symmetric construction, the off diagonal terms are identically zero.

5.2. Conjugate symmetric transmit waveforms

In this section, we look at waveforms that exhibit conjugate symmetry. An important aspect in the design of conjugate symmetric waveforms is their DFT (Discrete Fourier Transform) properties. Since the DFT of a conjugate symmetric sequence is real valued, the use of conjugate symmetric sequences enables  $2 \times 2$ ,  $4 \times 4$  and  $8 \times 8$  waveform scheduling according to OSTBC (Orthogonal Space-Time Block Codes) for real designs.

Consider the SRRC (Square Root Raised Cosine) quarter-band filter impulse response given by

$$p(t) = \frac{\frac{4\alpha t}{T} \cos\left(\frac{(1+\alpha)\pi t}{T}\right) + \sin\left(\frac{(1-\alpha)\pi t}{T}\right)}{\frac{\pi t}{T} \left[1 - \left(\frac{4\alpha t}{T}\right)^2\right]} \tag{55}$$

In order to make four conjugate symmetric waveforms using the SRRC, we sample this pulse with a sampling interval  $T_s = \frac{T}{4}$ . This gives us

$$p(n) = \frac{\alpha \cos\left((1 + \alpha)\frac{\pi}{4}n\right) + \sin\left((1 - \alpha)\frac{\pi}{4}n\right)}{n\frac{\pi}{4}(1 - (n\alpha)^2)} \tag{56}$$

The response with a roll-off factor of  $\alpha = 0.5$  is shown in Fig. 3(a). This waveform is then modulated by  $e^{j\frac{\pi}{4}n}$ ,  $e^{-j\frac{\pi}{4}n}$ ,  $e^{j\frac{3\pi}{4}n}$ , and  $e^{j\frac{-3\pi}{4}n}$  to get four quarter-band SRRC waveforms, given by

$$s_1(n) = p(n)e^{j\frac{\pi}{4}n}$$



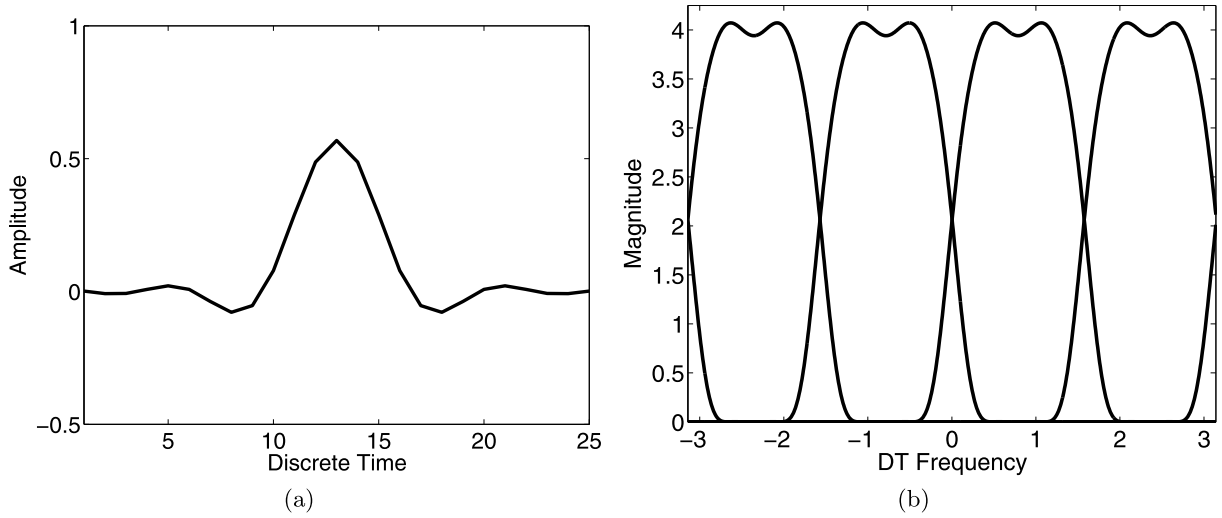


Fig. 3. (a) Impulse response of the quarter-band filter. (b) Frequency response of the four quarter-band filter waveforms.

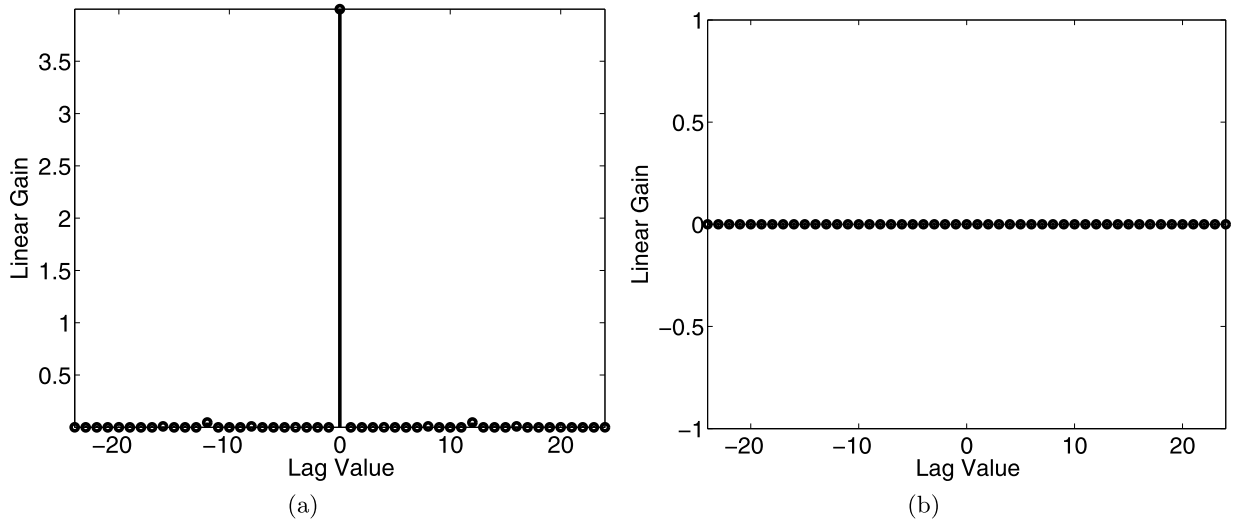


Fig. 4. (a) Main diagonal sequence is close to a delta function. (b) Off diagonal sequence is identically zero.

$$\begin{aligned}
 s_2(n) &= p(n)e^{-j\frac{\pi}{4}n} \\
 s_3(n) &= p(n)e^{j\frac{3\pi}{4}n} \\
 s_4(n) &= p(n)e^{-j\frac{3\pi}{4}n}
 \end{aligned} \tag{57}$$

The combined frequency response of these waveforms is shown in Fig. 3(b). The main and off diagonal sequences of the Key matrix for these waveforms are given in Figs. 4(a) and 4(b). We see from these figures that these waveforms are perfectly separable except for the negligible disturbance in the autocorrelation function around the lag values  $\pm 12$  which can be eliminated by making the sequences longer.

### 5.3. Combination of Golay codes and half band filters

In the previous section, we created waveforms with quarter-band filters that achieved perfect separation. In this section, we form transmit waveforms through the Kronecker product of Golay codes with half-band SRRC filters. The half-band SRRC waveform is obtained by sampling  $p(t)$  in (70) at  $T_s = \frac{T}{2}$ , i.e.,

$$p(n) = \frac{2\alpha \cos((1 + \alpha)\frac{\pi}{2}n) + \sin((1 - \alpha)\frac{\pi}{2}n)}{n\frac{\pi}{2}(1 - (2n\alpha)^2)} \tag{58}$$

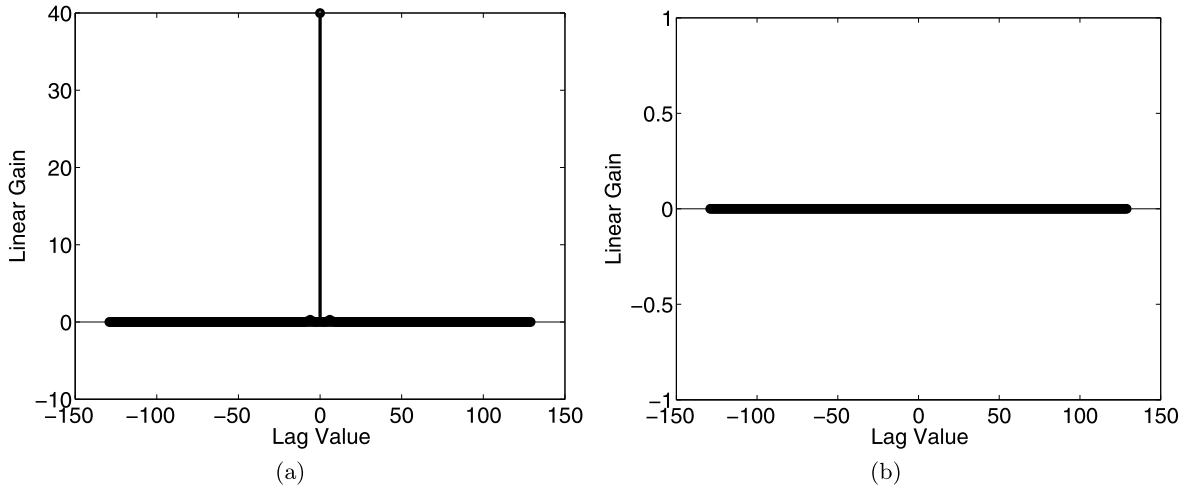


Fig. 5. (a) Main diagonal sequence resembles a delta function. (b) Off diagonal sequence is identically zero.

The two half-band SRRC waveforms are then obtained by modulating  $p(n)$  with  $e^{j\frac{\pi}{2}n}$  and  $e^{-j\frac{\pi}{2}n}$ , i.e.,

$$h_b^{(1)}(n) = p(n)e^{j\frac{\pi}{2}n} \tag{59}$$

$$h_b^{(2)}(n) = p(n)e^{-j\frac{\pi}{2}n} \tag{60}$$

The transmit waveforms are formed by the Kronecker product of these waveforms with the Golay complementary codes  $g_1(n)$  and  $g_2(n)$ , and are given by

$$\begin{aligned} s_1(n) &= g_1(n) \otimes h_b^{(1)}(n) \\ s_2(n) &= g_1(n) \otimes h_b^{(2)}(n) \\ s_3(n) &= g_2(n) \otimes h_b^{(1)}(n) \\ s_4(n) &= g_2(n) \otimes h_b^{(2)}(n) \end{aligned} \tag{61}$$

where  $g_i(n)$  are the Golay codes and  $h_i(n)$  are the half-band filters. The main and off diagonal sequences of the Key matrix are shown in Figs. 5(a) and 5(b). We see that the waveforms formed from the Kronecker product of Golay sequences with half-band filters possess excellent separation properties.

## 6. Doppler compensation

In this section, we develop a signal model that incorporates the effects of Doppler. We assume that the target is moving at a constant speed, which means that between any two PRIs, the Doppler shift would be constant.

### 6.1. Effects of Doppler

In the presence of Doppler, the received signal is given by

$$\mathbf{R}(n) = \mathbf{H}^T(n) * \mathbf{S}(n)\mathbf{D} + \mathbf{N}(n) \tag{62}$$

The Doppler shift matrix  $\mathbf{D}$  is given by

$$\mathbf{D} = \begin{bmatrix} 1 & 0 & 0 & 0 \\ 0 & e^{j\nu} & 0 & 0 \\ 0 & 0 & e^{j2\nu} & 0 \\ 0 & 0 & 0 & e^{j3\nu} \end{bmatrix} \tag{63}$$

where  $\nu$  is the phase shift due to Doppler from one PRI to the next. As in the case of negligible Doppler, we process the received waveform matrix as

$$\mathbf{R}(n) * \mathbf{S}^H(-n) = \mathbf{H}^T(n) * \mathbf{S}(n)\mathbf{D} * \mathbf{S}^H(-n) + \mathbf{N}(n) * \mathbf{S}^H(-n) \tag{64}$$

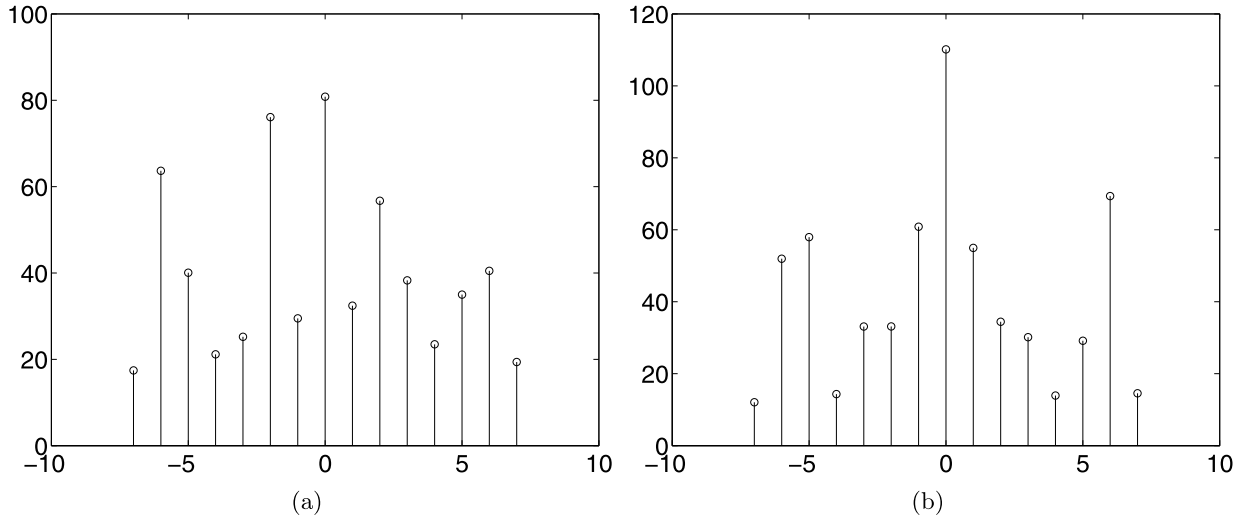


Fig. 6. Plot of the detection statistic in the presence of Doppler for (a) SNR = 5 dB. (b) SNR = 10 dB.

In the presence of non-trivial Doppler phase shift, the condition in (4) is not satisfied in general, i.e.,

$$\mathbf{S}(n)\mathbf{D} * \mathbf{S}^H(-n) \neq \alpha \mathbf{I} \delta(n) \tag{65}$$

and unambiguous range resolution is no longer possible. To illustrate this, we plot the detection statistic  $\|\mathbf{R}(n) * \mathbf{S}^H(-n)\|^2$  in Fig. 6 for target SNR of 5 dB and 10 dB. As we can see, the presence of Doppler makes it impossible to detect the target. We now develop a new method for eliminating this problem.

### 6.2. Doppler processing

Consider the matrix

$$\mathbf{\Gamma}(n) = \mathbf{R}(n) * \mathbf{S}^H(-n) \tag{66}$$

Each term of this matrix is a sum of four individual convolution sequences, and the  $i$ th row corresponds to the output of the received symbols on antenna  $i$ . Now, consider the matrix  $\mathbf{Y}_i$ , given by

$$\mathbf{Y}_i(n) = \begin{bmatrix} r_{i1}(n) * s_1^*(-n) & r_{i1}(n) * -s_2^*(-n) & r_{i1}(n) * -s_3^*(-n) & r_{i1}(n) * -s_4^*(-n) \\ r_{i2}(n) * s_2(n) & r_{i2}(n) * s_1(n) & r_{i2}(n) * s_4(n) & r_{i2}(n) * -s_3(n) \\ r_{i3}(n) * s_3^*(-n) & r_{i3}(n) * -s_4^*(-n) & r_{i3}(n) * s_1^*(-n) & r_{i3}(n) * s_2^*(-n) \\ r_{i4}(n) * s_4(n) & r_{i4}(n) * s_3(n) & r_{i4}(n) * -s_2(n) & r_{i4}(n) * s_1(n) \end{bmatrix} \tag{67}$$

where column  $j$  is formed from the individual convolution sequences which add up to give the  $ij$ th term in  $\mathbf{\Gamma}(n)$ , i.e.

$$\mathbf{\Gamma}_i = \mathbf{w}^T \mathbf{Y}_i(n) \tag{68}$$

where  $\mathbf{\Gamma}_i$  is the  $i$ th row of  $\mathbf{\Gamma}$ , and

$$\mathbf{w} = [1 \quad 1 \quad 1 \quad 1]^T \tag{69}$$

**Theorem 6.1.**  $\forall n \neq 0, -(N_c - 1) \leq n \leq (N_c - 1)$ , the matrix  $\mathbf{Y}_i(n)$  is singular.

**Proof.** See Appendix B.  $\square$

This means that for  $n \neq 0$ , the matrices  $\mathbf{Y}_i$  are singular, and the vector producing the desired output lies in the null-space of these matrices. Also, because of the similar waveform structure, the matrices  $\mathbf{Y}_i$  share the same null-space, and we can work with concatenated matrix given by

$$\mathbf{Y}_C(n) = [\mathbf{Y}_1(n) \quad \mathbf{Y}_2(n) \quad \mathbf{Y}_3(n) \quad \mathbf{Y}_4(n)] \tag{70}$$

Defining

$$\mathbf{w}_D = [1 \quad e^{j\nu} \quad e^{2j\nu} \quad e^{3j\nu}]^T \quad (71)$$

We can easily verify that

$$\mathbf{w}_D^H \mathbf{Y}_C(n) = \mathbf{w}_D^H [\mathbf{Y}_1(n) \quad \mathbf{Y}_2(n) \quad \mathbf{Y}_3(n) \quad \mathbf{Y}_4(n)] = \gamma \mathbf{vec}(\mathbf{H}^T)^T \quad (72)$$

Which means that our desired processing vector lies in the null-space of the received matrix for values of  $n$  that do not correspond to the true target delay. Now, since we don't know the value of  $n$  for which  $\mathbf{Y}_C(n)$  is non-singular, i.e. the true target delay, we cannot just find the null-space vector at every  $n$ . To get around this problem of  $\mathbf{w}_D$  not being in the null-space of  $\mathbf{Y}_C(n)$  at the correct target delay, we adopt an approach in which we try to nullify the effect of  $\mathbf{Y}_C(n)\delta(n)$  on the null space, where  $\delta(n)$  specifies the fact that the correct target delay is assumed to be 0. From this point onwards, we'll work with the concatenated matrix  $\mathbf{Y}_C(n)$  to take advantage of the fact that since all antennas share the same null-space vector, we can form an average correlation matrix using this concatenated matrix to reduce the effects of noise. To counter the effect of  $\mathbf{Y}_C(n)\delta(n)$  on the null-space, instead of working with a single chip interval, we take a length  $2q + 1$  window and form the matrix

$$\mathbf{X}_C(n') = [\mathbf{Y}_C(n' - q) \quad \dots \quad \mathbf{Y}_C(n') \quad \dots \quad \mathbf{Y}_C(n' + q)] \quad (73)$$

The correlation function of  $\mathbf{X}_C(n')$  is given by

$$\mathbf{R}_{X_C X_C}(n') = \mathbf{X}_C(n') \mathbf{X}_C^H(n') \quad (74)$$

The length  $2q + 1$  window is formed to exploit the fact that if we could subtract of the effect of  $\mathbf{Y}_C(n)\delta(n)$  on the null space of  $\mathbf{R}_{X_C X_C}(n')$ , we could still process the returns in a way that would allow us to detect the correct target delay. To do this, we find the SVD of

$$\mathbf{R}_{X_C X_C}(n') - \mathbf{Y}_C(k) \mathbf{Y}_C^H(k) \quad (75)$$

for each value of  $k$  such that  $n' - q \leq k \leq n' + q$  and store the singular vector associated with the smallest eigenvalue. Note that out of the  $2q + 1$  singular vectors that we store for each  $n$ , there is at most one singular vector that corresponds to  $\mathbf{Y}_C(n)\delta(n)$  and this happens whenever  $0 \in \{n - q, \dots, n + q\}$ . Since the inclusion of  $\mathbf{Y}_C(n)\delta(n)$  changes the null-space structure, we take a dot product of each of the  $2q + 1$  singular vectors with the other  $2q$  singular vectors, and choose the one that has the smallest dot product with the rest of the vectors. Let  $\mathbf{U}_{\min}(n')$  be the matrix with the  $2q + 1$  singular vectors as columns. The dot product is given by

$$\mathbf{M}(n') = \mathbf{U}_{\min}^H(n') \mathbf{U}_{\min}(n') \quad (76)$$

We can write  $\mathbf{M}(n')$  as

$$\mathbf{M}(n') = \begin{bmatrix} \mathbf{m}_1 \\ \vdots \\ \mathbf{m}_{2q+1} \end{bmatrix} \quad (77)$$

The index of the singular vector of interest is given by

$$l = \arg \min_i \|\mathbf{m}_i\| \quad (78)$$

To check the presence of target in the delay bin  $n'$ , we process the vector  $\mathbf{Y}_C(n')$  as

$$z(n') = \|\mathbf{u}_l^H(n') \mathbf{Y}_C(n')\| \quad (79)$$

If the target is present, we should expect a sharp peak, while the magnitude of  $z(n')$  for all other values of  $n'$  should be small.

## 7. Simulation results

We simulated a  $4 \times 4$  system using Golay complementary sequences of length  $N_c = 10$ . The channel entries are i.i.d. complex Gaussian with unit variance. The simulation results are plotted in Figs. 7, 8 and 9 and we use a window length of  $2q + 1 = 5$ . For the single target case, we plot  $z(n)$  for target SNR values of 5 and 10 dB and a Doppler shift of  $\nu = \pi/3$  in Fig. 7. For the case of multiple targets, the simulation results show that if the separation in chip intervals is greater than  $N_c$  or if the targets are moving with approximately the same speed with a separation greater than window length  $2q + 1$ , we are able to resolve targets moving at different speeds using our technique. Fig. 8 shows the system performance for the case when two targets introducing the same Doppler shift of  $\pi/3$  and are separated by more than window length. Fig. 9

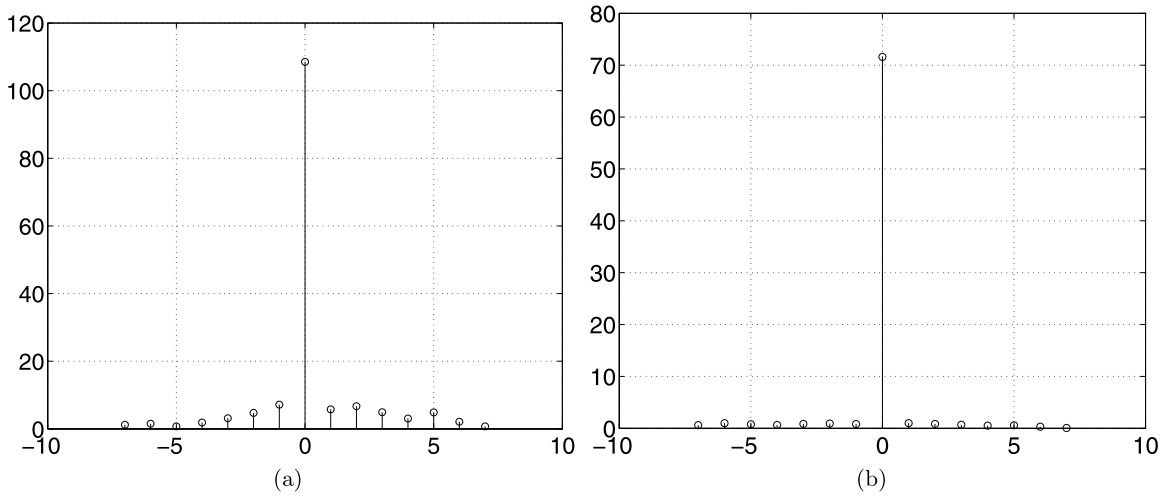


Fig. 7. (a) Plot of the detection statistic for a Doppler shift of  $\pi/3$  for (a) SNR = 5 dB and (b) SNR = 10 dB.

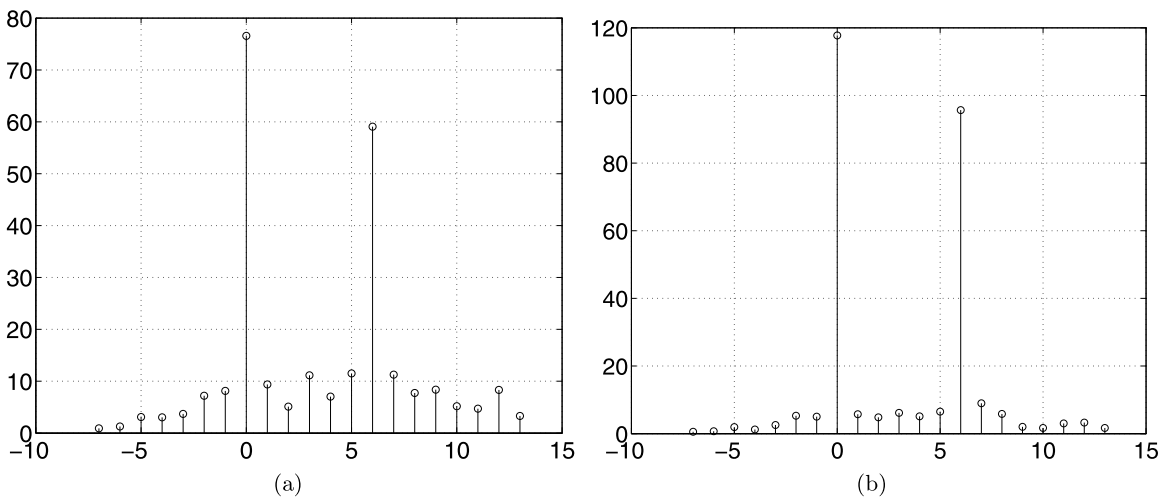


Fig. 8. Plot of the detection statistic for two target with the same Doppler shift of  $\pi/3$  for (a) SNR = 5 dB and (b) SNR = 10 dB.

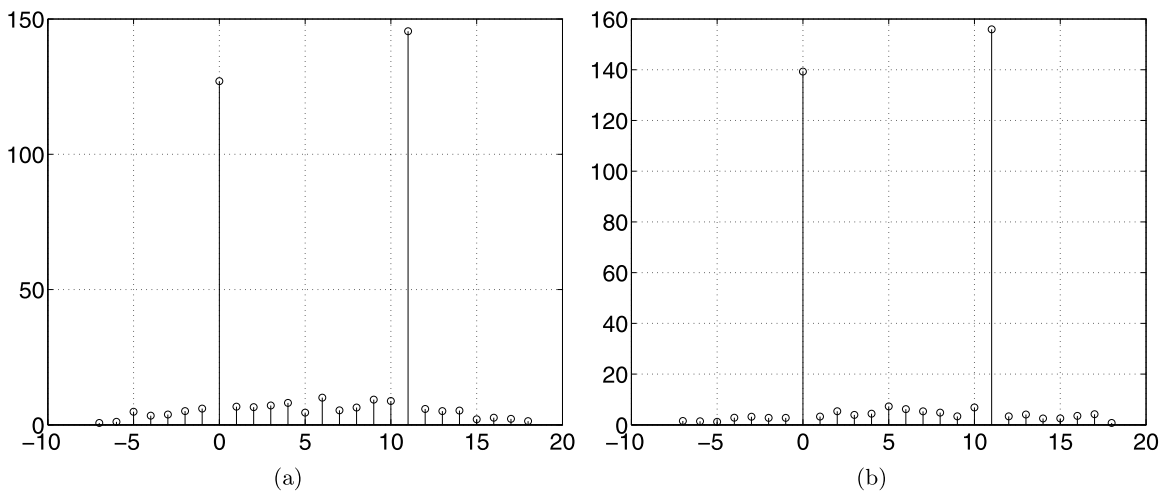


Fig. 9. Plot of the detection statistic for two targets with respective Doppler shifts of  $\pi/3$  and  $2\pi/3$  for (a) SNR = 5 dB and (b) SNR = 10 dB.

shows the contrast in system performance with the two targets moving at different velocities, introducing Doppler shifts of  $\pi/3$  and  $2\pi/3$  respectively while separated in time by more than the code length  $N_c = 10$ . As we can see from these figures, our Doppler processing technique performs very well for compensating the Doppler shift and correctly determining the target delay.

## 8. Extension to antenna arrays of arbitrary size

So far, we have only consider the  $2 \times 2$  and  $4 \times 4$  symmetrical systems. We now extend these ideas to transmit and receive arrays of arbitrary sizes. Consider a system with  $N_T$  transmit and  $N_R$  receive antennas. Let  $m_1, m_2$  be such that  $2^{m_1-1} < N_T \leq 2^{m_1}$  and  $2^{m_2-1} < N_R \leq 2^{m_2}$  where  $m_1$  and  $m_2$  are positive integers. There are  $N_T$  channel coefficients between the transmit array and each element of the receive array. Now, using the ideas developed earlier, we know that a waveform matrix exists for the  $2^{m_1} \times 2^{m_1}$  system. From this matrix, we extract a sub-matrix of dimension  $N_T \times 2^{m_1}$  and we call this matrix  $\tilde{\mathbf{S}}_{N_T}(\omega)$ . Now, since each row of the matrix  $\mathbf{S}_{2^{m_1}}$  is orthogonal to every other row, the sub-matrix  $\tilde{\mathbf{S}}'_{N_T}(\omega)$  is also orthogonal, i.e.

$$\tilde{\mathbf{S}}_{N_T}(\omega)\tilde{\mathbf{S}}_{N_T}^H(\omega) = 2^{m_1}\mathbf{I}_{N_T} \quad (80)$$

Therefore, we can process the received space–time waveform matrix at every antenna with the matrix  $\tilde{\mathbf{S}}_{N_T}^H(\omega)$ , and we'll be able to isolate the channel gains corresponding to that antenna. Therefore, this ideas presented in this paper are applicable to any general antenna array of arbitrary dimensions. As an example, consider the  $3 \times 3$  case. To make the ideas in this paper work for this system, we would take the first three rows of the matrix in (26), and use that as our transmitted waveform matrix. It is easy to verify that the shortened matrix still satisfies the perfect reconstruction and separation properties.

## 9. Summary

We have developed waveform design strategies for MIMO radar in the delay domain, where we have derived some of the conditions for perfect waveform separation and reconstruction at the receiving end. Examples of diversity waveforms for  $2 \times 2$  and  $4 \times 4$  have been provided and some new waveforms designs have been proposed that allow for near perfect separation and reconstruction at the receiver. We saw that Kronecker products of waveform sequences possess some desirable properties that make them suitable for use in radar and active sensing applications. We then introduced Doppler into the system, and developed a technique for doing accurate target ranging in the presence of Doppler. The technique is based on finding the null-space of the waveform matrix after matched filtering at the receiver, and then using an appropriate vector from the null-space to process the matched filtered received waveform. We provide simulation results using Golay complementary sequences that show how our proposed technique minimizes the effects of Doppler and makes accurate target ranging possible over a wide range of target SNRs for both the single and the multi-target scenarios. In the future, we intend to provide a theoretical analysis of the detection performance and explore further enhancements in delay–Doppler resolution.

## Appendix A. Proof of Theorem 5.1

Since

$$z(n) = x(n) \otimes y(n) \Rightarrow r_{zz}(m) = r_{xx}(m) \otimes_N r_{yy}(m) \quad (81)$$

we have that

$$\begin{aligned} r(m) &= (r_{\varepsilon_1\varepsilon_1}(m) \otimes_N r_{\varepsilon_3\varepsilon_3}(m)) + (r_{\varepsilon_1\varepsilon_1}(m) \otimes_N r_{\varepsilon_4\varepsilon_4}(m)) + (r_{\varepsilon_2\varepsilon_2}(m) \otimes_N r_{\varepsilon_3\varepsilon_3}(m)) + (r_{\varepsilon_2\varepsilon_2}(m) \otimes_N r_{\varepsilon_4\varepsilon_4}(m)) \\ &= (r_{\varepsilon_1\varepsilon_1}(m) \otimes_N (r_{\varepsilon_3\varepsilon_3}(m) + r_{\varepsilon_4\varepsilon_4}(m))) + (r_{\varepsilon_2\varepsilon_2}(m) \otimes_N (r_{\varepsilon_3\varepsilon_3}(m) + r_{\varepsilon_4\varepsilon_4}(m))) \\ &= N_1(r_{\varepsilon_1\varepsilon_1}(m) \otimes_N \delta(m)) + N_1(r_{\varepsilon_2\varepsilon_2}(m) \otimes_N \delta(m)) \\ &= N_1((r_{\varepsilon_1\varepsilon_1}(m) + r_{\varepsilon_2\varepsilon_2}(m)) \otimes_N \delta(m)) \\ &= N_1 N_2 (\delta(m) \otimes_N \delta(m))(m) \\ &= N_1 N_2 \delta(m) \end{aligned} \quad (82)$$

## Appendix B. Proof of Theorem 6.1

To prove this, we need to show that  $\exists \mathbf{w} \in \mathbb{C}^4$  s.t.  $\mathbf{w} \neq \mathbf{0}$  and  $\mathbf{w}^H \mathbf{Y}_i(n) = \mathbf{0} \forall n \neq 0, -(N_c - 1) \leq n \leq (N_c - 1)$ . Consider the case of negligible Doppler first, and define

$$\mathbf{w} = [1 \ 1 \ 1 \ 1]^T \quad (83)$$

Now, in order to prove that the matrix  $\mathbf{Y}_i$  is singular, we need to show that

$$\mathbf{w}^T \mathbf{Y}_i(n) = 0 \quad \forall n \neq 0 \quad (84)$$

However, we know that

$$\mathbf{w}^T \mathbf{Y}_i(n) = \Gamma_i(n) \quad (85)$$

and for the case of negligible Doppler, we have

$$\Gamma(n) = 0 \quad \forall n \neq 0 \quad (86)$$

Therefore, for  $n \neq 0$ , (84) holds, and the matrix  $\mathbf{Y}_i(n)$  is singular. Now, we know that  $\mathbf{Y}_i(n)$  is formed from  $\mathbf{S}(n)$  and since multiplication by a diagonal matrix does not change the subspace structure, the theorem holds when we multiply  $\mathbf{S}(n)$  by  $D$ , and therefore, the matrix  $\mathbf{Y}_i(n)$  is singular for non-negligible Doppler as well.

## References

- [1] N. Levanon, Radar Principles, Wiley-Interscience, 2001.
- [2] A. Farina, Antenna Based Signal Processing Techniques for Radar Systems, Artech House, 1992.
- [3] H. Wang, L. Cai, On adaptive spatio-temporal processing for airborne surveillance radar systems, IEEE Trans. Aerospace Electron. Syst. 30 (1994) 660–669.
- [4] J. Ward, Cramer–Rao bounds for target Doppler and angle estimation with space–time adaptive processing in radar, in: Proc. 29th Asilomar Conference on Signals, Syst. Comput., 1995, pp. 1198–1202.
- [5] E. Fishler, A. Haimovich, R. Blum, D. Chizhik, L. Cimini, R. Valenzuela, MIMO radar: an idea whose time has come, in: Proc. IEEE Radar Conference, 2004, pp. 71–78.
- [6] H. Schulze, C. Lueders, Theory and Applications of OFDM and CDMA: Wideband Wireless Communications, Wiley, 2005.
- [7] S.D. Howard, A.R. Calderbank, W. Moran, A simple polarization diversity scheme for radar detection, in: Proc. of Second Int. Conference on Waveform Diversity and Design, 2006, pp. 22–27.
- [8] M.J.E. Golay, Static multislit spectrometry and its applications to the panoramic display of infrared spectra, J. Opt. Soc. Amer. 41 (1951) 468–472.
- [9] S. Alamouti, A simple transmit diversity technique for wireless communications, IEEE J. Select. Areas Commun. 16 (1998) 1451–1458.
- [10] A. Pezeshki, A.R. Calderbank, W. Moran, S.D. Howard, Doppler resilient Golay complementary waveforms, IEEE Trans. Inform. Theory 54 (9) (2008) 4254–4266.
- [11] E. Prouhet, Mémoire sur quelques relations entre les puissances des nombres, C. R. Acad. Sci. Paris Sér. I 33 (1851) 225.
- [12] M. Morse, Recurrent geodesics on a surface of negative curvature, Trans. Amer. Math. Soc. 22 (1921) 84–100.
- [13] J.P. Allouche, J. Shallit, Automatic Sequences: Theory, Applications, Generalizations, Cambridge Univ. Press, 2003.
- [14] J.P. Allouche, J. Shallit, The ubiquitous Prouhet–Thue–Morse sequence, in: T.H.C. Ding, H. Niederreiter (Eds.), Sequences and Their Applications, Proc. SETA'98, Springer-Verlag, 1999, pp. 1–16.
- [15] D.H. Lahmer, The Tarry–Escott problem, Scripta Math. 13 (1947) 37–41.

**T.R. Qureshi** received his B.S. in Electrical Engineering from the University of Engineering and Technology, Lahore in 2002, M.S. in Computer Engineering from Lahore University of Management Sciences in 2005, and M.S. in Electrical Engineering from the University of Wisconsin, Madison in 2006. Since 2006, he is pursuing Ph.D. in Electrical Engineering at Purdue University, West Lafayette, IN. His research interests lie in the areas of signal processing, waveform design, and improving delay–Doppler resolution in multiantenna sensing systems.

**Michael D. Zoltowski** was born in Philadelphia, PA, on August 12, 1960. He received both the B.S. and M.S. degrees in Electrical Engineering with highest honors from Drexel University in 1983 and the Ph.D. in Systems Engineering from the University of Pennsylvania in 1986. In Fall 1986, he joined the faculty of Purdue University. In 2001, he was named a University Faculty Scholar. He currently holds an Endowed Chair position as the Thomas J and Wendy Engibous Professor of Electrical and Computer Engineering. In this capacity, he was the Ruth and Joel Spira Outstanding Teacher Award for 1990–1991 and the 2001–2002 Wilfred Hesselberth Award for Teaching Excellence. In 2001, he was named a University Faculty Scholar by Purdue University.

Dr. Zoltowski is the recipient of a 2002 Technical Achievement Award from the IEEE Signal Processing Society. In addition, he selected as a 2003 Distinguished Lecturer for the IEEE Signal Processing Society. He is a Fellow of IEEE. He was a recipient of the 2006 Distinguished Alumni Award from Drexel University.

Dr. Zoltowski is a co-recipient of the IEEE Communications Society 2001 Leonard G. Abraham Prize Paper Award in the Field of Communications Systems. He was also the recipient of the IEEE Signal Processing Society's 1991 Paper Award, "The Fred Eilersick MILCOM Award for Best Paper in the Unclassified Technical Program" at the 1998 IEEE Military Communications Conference, and a Best Paper Award at the 2000 IEEE International Symposium on Spread Spectrum Techniques and Applications.

In addition, from 1998 to 2001, Dr. Zoltowski was an elected Member-at-Large of the Board of Governors and Secretary of the IEEE Signal Processing Society. From 2003 to 2005, he served on the Awards Board of the IEEE Signal Processing Society and served as the Area Editor in charge of Feature Articles for the IEEE Signal Processing Magazine. Within the IEEE Signal Processing Society, he has been a member of the Technical Committee for the Statistical Signal and Array Processing Area, the Technical Committee for DSP Education and the Technical Committee on Signal Processing for Communications (SPCOM).

From 2003 to 2004, he served as Vice-Chairman of the Technical Committee on Sensor and Multichannel (SAM) Processing, and currently serves as Chairman. He has served as an associate editor for both the IEEE Transactions on Signal Processing and the IEEE Communications Letters. He was Technical Co-Chairman of the 2006 IEEE Sensor Array and Multichannel Workshop.

**Robert Calderbank** received the B.Sc. degree in 1975 from Warwick University, England, the M.Sc. degree in 1976 from Oxford University, England, and the Ph.D. degree in 1980 from the California Institute of Technology, all in mathematics.

Dr. Calderbank is the Dean of Natural Sciences at Duke University. Before that, he was the Professor of Electrical Engineering and Mathematics at Princeton University where he directs the Program in Applied and Computational Mathematics. He joined Bell Telephone Laboratories as a Member of Technical Staff in 1980, and retired from AT&T in 2003 as Vice President of Research. Dr. Calderbank has made significant contributions to a wide range of research areas, from algebraic coding theory and quantum computing to wireless communication and active sensing.

Dr. Calderbank served as Editor in Chief of the IEEE Transactions on Information Theory from 1995 to 1998, and as Associate Editor for Coding Techniques from 1986 to 1989. He was a member of the Board of Governors of the IEEE Information Theory Society from 1991 to 1996 and began a second term in 2006. Dr. Calderbank was honored by the IEEE Information Theory Prize Paper Award in 1995 for his work on the Z4 linearity of Kerdock and Preparata Codes (joint with A.R. Hammons Jr., P.V. Kumar, N.J.A. Sloane, and P. Sole), and again in 1999 for the invention of space–time codes (joint with V. Tarokh and N. Seshadri). He received the 2006 IEEE Donald G. Fink Prize Paper Award and the IEEE Millennium Medal, and was elected to the US National Academy of Engineering in 2005.

**Ali Pezeshki** received the B.Sc. and M.Sc. degrees in Electrical Engineering from the University of Tehran, Tehran, Iran, in 1999 and 2001, respectively. He earned his Ph.D. degree in Electrical Engineering at Colorado State University in 2004. In 2005, he was a postdoctoral research associate with the Electrical and Computer Engineering Department at Colorado State University. From January 2006 to August 2008, he was a postdoctoral research associate with The Program in Applied and Computational Mathematics at Princeton University. Since August 2008, he has been an assistant professor with the Department of Electrical and Computer Engineering, Colorado State University, Fort Collins, CO. His research interests are in statistical signal processing and coding theory and their applications to distributed sensing, wireless communication, active/passive sensing, data networking, and bioimaging.